Hydrothermal Synthesis, Crystal Structures, Spectroscopic, and Magnetic Properties of Two New Organically Templated Monodimensional Phosphite Compounds: $(C_2H_{10}N_2)[M(HPO_3)F_3]$, M = V(III) and Cr(III)

Sergio Fernández,[†] José L. Mesa,*[,†] José L. Pizarro,[‡] Luis Lezama,[†] María I. Arriortua,[‡] and Teófilo Rojo*[,†]

Departamento de Química Inorgánica and Mineralogía-Petrología, Facultad de Ciencias, Universidad del País Vasco, Apdo. 644, E-48080 Bilbao, Spain

Received November 19, 2002. Revised Manuscript Received January 6, 2003

The organically templated $(C_2H_{10}N_2)[M(HPO_3)F_3]$, M = V(III) and Cr(III), compounds have been synthesized under mild hydrothermal conditions. The crystal structures have been determined from X-ray single-crystal diffraction data. The compounds crystallize in the $P2_12_12_1$ orthorhombic space group. The unit-cell parameters are $a = 12.809(2)$ Å, $b = 9.518(1)$ Å, $c = 6.440(1)$ Å for the vanadium phase, and $a = 12.801(2)$ Å, $b = 9.337(1)$ Å, $c = 6.508(1)$ Å for the chromium compound, with $Z = 4$. The crystal structure of these compounds consists of $[M(HPO_3)F_3]^{2-}$ anionic chains. The ethylenediammonium cations are placed in the space delimited by three different chains. The metallic ions are interconnected by the pseudopyramidal $(HPO_3)^{2-}$ phosphite oxoanions and the fluorine anions, adopting a slightly distorted octahedral geometry. The IR and Raman spectra show the bands corresponding to the phosphite oxoanion and ethylenediammonium cation. The *Dq* and Racah (*B* and *C*) parameters have been calculated from the diffuse reflectance spectra in the visible region. The ESR spectra of the chromium(III) compound are isotropic with a *g* value of 1.97. Magnetic measurements indicate the existence of antiferromagnetic interactions.

Introduction

Compounds with open-framework structures are of great interest in material science, as well as in chemistry, because of their applications as catalysts, ion-exchangers, or molecular sieves.[1] The organically templated inorganic networks now cover a remarkable range of compositions and structures.[2] The use of hydrothermal techniques for the synthesis of these novel inorganic materials with open architectures has grown steadily during the past decade. This synthetic approach generally employs the use of an organic amine, which is accommodated within the cavities and channels of these open structures. The introduction of fluoride ions, which act both as a mineralizer and as a connector between the metal atoms, strongly influences the formation of the framework solid of these materials.[3]

Altough attention focused initially on the phosphates of aluminum and gallium because of their structural similarities to zeolites and clays, numerous open-framework transition-metal phosphates are now also known.[1] Besides, in the past few years considerable efforts have been devoted to designing open-framework inorganic materials other than phosphates, such as chalcogenides, pnictides, cyanides, and thiopnictides.[4,5] The possibilities of incorporating phosphorus(III) as pseudo-pyramidal $(HPO_3)^{2-}$ hydrogen phosphite into extended structures templated by inorganic alkaline earth cations were explored a few years ago.[6] However, the inorganic−organic hybrid phosphites with metallic transition elements have not been extensively studied, and only compounds with the V(IV), Co(II), Mn(II), Fe(III), and V(III) cations are known.[7] To complete the knowledge about this type of microporous material incorporating metallic magnetic cations belonging to the

* To whom correspondence should be addressed. Phone: 34-946012458. Fax: 34-944648500; E-mail: qiproapt@lg.ehu.es.
[†] Departamento de Química Inorgánica.
[‡] Departamento de Mineralogía-Petrología.

(1) Cheetham, A. K.; Ferey, G.; Loiseau, T. *Angew. Chem., Int. Ed.* **1999**, *38*, 3268.
(2) Ferey, G. *Chem. Mater.* **2001**, *13*, 3084.
(3) Ferey, G.; Loiseau, T.; Riou, D. *Advanced Inorganic Fluorides: Synthesis, Characterization and Applications*; Elsevier Science: New York, 2000; Chapter 7.
(4) Bowes, C. L.; Ozin, G. A. *Adv. Mater.* **1996**, *8*, 13.
(5) Conard, O.; Jansen, C.; Krebs, B. *Angew. Chem., Int. Ed.* **1998**, *37*, 3208.
(6) (a) Shieh, M.; Martin, K. J.; Squattrito, P. J.; Clearfield, A. *Inorg. Chem.* **1990**, *29*, 958. (b) Sapiña, F.; Gomez, P.; Marcos, M. D.; Amoros, P.; Ibañez, R.; Beltran, D. *Eur. J. Solid State Inorg. Chem.* **1989**, *26*, 603. (c) Marcos, M. D.; Amoros, P.; Beltran, A.; Martinez, R.; Attfield, J. P. *Chem. Mater.* **1993**, *5*, 121. (d) Attfield, M. P.; Morris, R. E.; Cheetham, A. K. *Acta Crystallogr.* **1994**, *C50*, 981. (e) Marcos, M. D.; Amoros, P.; Le Bail, A. *J. Solid State Chem.* **1993**, *107*, 250.
(7) (a) Bonavia, G.; DeBord, J.; Haushalter, R. C.; Rose, D.; Zubieta, J. *Chem. Mater.* **1995**, *7*, 1995. (b) Fernandez, S.; Mesa, J. L.; Pizarro, J. L.; Lezama, L.; Arriortua, M. I.; Olazcuaga, R.; Rojo, T. *Chem. Mater.* **2000**, *12*, 2092. (c) Fernandez, S.; Pizarro, J. L.; Mesa, J. L.; Lezama, L.; Arriortua, M. I.; Olazcuaga, R.; Rojo, T. *Inorg. Chem.* **2001**, *40*, 3476. (d) Fernandez, S.; Pizarro, J. L.; Mesa, J. L.; Lezama, L.; Arriortua, M. I.; Rojo, T. *Int. J. Inorg. Mater.* **2001**, *3*, 331. (e) Fernandez, S.; Mesa, J. L.; Pizarro, J. L.; Lezama, L.; Arriortua, M. I.; Rojo, T. *Chem. Mater.* **2002**, *14*, 2300.

10.1021/cm021361b CCC: $25.00 © 2003 American Chemical Society
Published on Web 02/14/2003

first series of transition elements we have synthesized the phosphites of formula $(C_2H_{10}N_2)[M(HPO_3)F_3]$, where M is V(III) and Cr(III). The crystal structure of these compounds and the spectroscopic and magnetic properties are also reported. A non-organically templated terephthalate chromium(III) compound has been recently reported.[8] However, the $(C_2H_{10}N_2)[Cr(HPO_3)F_3]$ phase is the first organically templated inorganic−organic hybrid compound which incorporates the chromium(III) cation into the M−O−P system by using hydrothermal techniques.[9]

Experimental Section

Synthesis and Characterization. The $(C_2H_{10}N_2)[M(HPO_3)F_3]$ [M = V (**1**) and Cr (**2**)] compounds were prepared under mild hydrothermal conditions. The starting reagents were V_2O_5, or $Cr(NO_3)_3{\cdot}9H_2O$, H_3PO_3, ethylenediamine, and HF in a molar ratio of 1:29:60:75 or 1:6:6:11 for phases (**1**) and (**2**), respectively. These reaction mixtures in a volume of 30 mL of water/ethanol 1.2:1 and 1:1 for (**1**) and (**2**), respectively, were stirred up to homogeneity. After that, they were placed in a PTFE-lined stainless steel pressure vessel (fill factor 75%) and heated at 170 °C for 5 days, followed by slow cooling to room temperature. The pH of the mixtures did not show any appreciable change during the hydrothermal reactions and remained at approximately 6.0 for (**1**), and 2 for (**2**). The compounds were obtained as green single crystals. The percentage of the elements in the products was calculated by inductively coupled plasma atomic emission spectroscopy (ICP−AES) and C, H, N elemental analysis. Fluorine content was determined by using a selective electrode. Found: V, 20.0; P, 12.0; C, 9.3; H, 4.2; N, 10.8; F, 22.2. $(C_2H_{10}N_2)[V(HPO_3)F_3]$ requires V, 20.2; P, 12.3; C, 9.5; H, 4.4; N, 11.1; F, 22.6. Found: Cr, 20.1; P, 12.0; C, 9.3; H, 4.1; N, 10.8; F, 22.0. $(C_2H_{10}N_2)[Cr(HPO_3)F_3]$ requires Cr, 20.5; P, 12.2; C, 9.5; H, 4.3; N, 11.1; F, 22.5. The densities were measured by flotation in mixtures of $CHCl_3/CHBr_3$. The values are 2.09(1) and 2.11(1) $g{\cdot}cm^{-3}$ for the vanadium and chromium compounds, respectively.

Thermogravimetric analysis was carried out under air atmosphere in a SDC 2960 Simultaneous DSC-TGA TA instrument. Crucibles containing ca. 20 mg of sample were heated at 5 $°C{\cdot}min^{-1}$ in the temperature range 30−800 °C. The decomposition curve of $(C_2H_{10}N_2)[V(HPO_3)F_3]$ reveals a mass loss between 300 and 360 °C of approximately 25.5% which agrees well with that calculated for the ethylenediammonium cation (24.6%). An additional weight loss was observed in the 360−680 °C range. This loss can be associated with the elimination of the fluorine anions together with the formation of $(VO)_2(P_2O_7)$.[10] Above 680 °C a slight increase of weight is observed. This fact was related to the oxidation process from $(VO)_2(P_2O_7)$ to $(VO)(PO_4)$.[10] The residue obtained at 800 °C remained pasted to the crucible and it was not possible to identify it by X-ray powder diffraction. The decomposition process of $(C_2H_{10}N_2)[Cr(HPO_3)F_3]$ between 300 and 540 °C takes place in three superimposed steps with different speed. The mass loss is approximately 40.0% in good agreement with the elimination of the ethylenediammonium together with a percentage of the fluorine anions (calc. 47.0%). Above 540 °C additional loss mass was not observed. The final residue obtained from the thermogravimetric analysis at 800 °C was amorphous.

The thermal behavior of the $(C_2H_{10}N_2)[M(HPO_3)F_3]$ (M = V and Cr) compounds was also studied by using time-resolved X-ray thermodiffractometry in air atmosphere. A Philips X'PERT automatic diffractometer (Cu Kα radiation) equipped with a variable-temperature stage (Paar Physica TCU2000) with a Pt sample holder was used in the experiment. The powder patterns were recorded in 2θ steps of 0.02° in the range $5 \le 2\theta \le 45$ °, counting for 1 s per step and increasing the temperature at 5 $°C{\cdot}min^{-1}$ from room temperature up to 800 °C. $(C_2H_{10}N_2)[V(HPO_3)F_3]$ is stable up to 255 °C and the intensity of the monitored (200) peak at $2\theta = 13.7°$ remains practically unchanged (Figure 1a). After that temperature, a rapid decrease of the crystallinity of the compound takes place and it becomes finally amorphous. Thus, in the 255−450 °C range no peaks were observed in the X-ray patterns. These results indicate the existence of collapse of the crystal structure of this compound with the loss of the ethylenediammonium cation. The thermodiffractograms recordered in the 450−480 °C range show peaks corresponding to the ω-$VO(PO_4)$ phase [$P4/mmm$ space group with $a = 6.839(1)$ Å, $c = 8.420(1)$ Å].[11a] Above this temperature the β-$VO(PO_4)$ phase is formed [$Pnma$ space group with $a = 7.78(1)$ Å, $b = 6.13(1)$ Å, $c = 6.97(1)$ Å].[11b] This phase gives rise to an amorphous compound at temperatures higher than 705 °C. The thermodiffractograms of $(C_2H_{10}N_2)[Cr(HPO_3)F_3]$ indicate that this compound is stable up to 285 °C, with the (200) peak at $2\theta = 13.7°$ remaining practically unchanged. The calcination of the organic cation takes place at higher temperatures, giving rise to an amorphous residue. This residue does not change into crystalline phases when the temperature is additionally increased until 800 °C (Figure 1b).

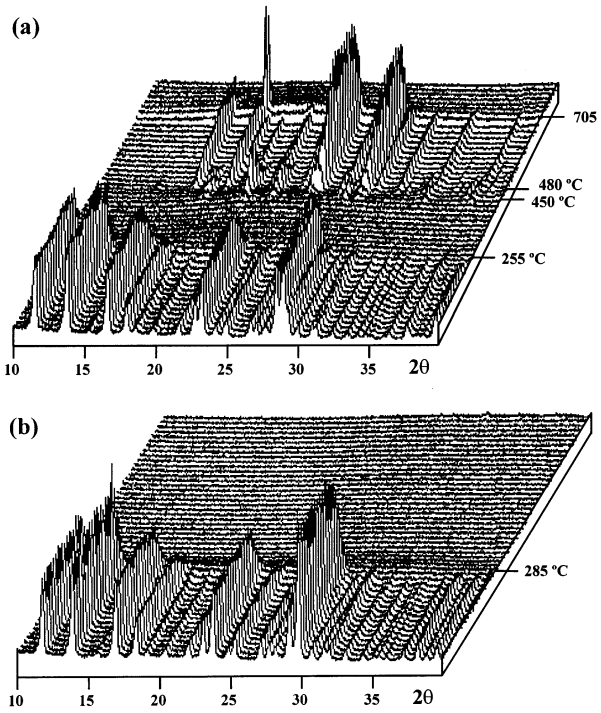

Figure 1. Thermodiffractograms of (a) $(C_2H_{10}N_2)[V(HPO_3)F_3]$ and (b) $(C_2H_{10}N_2)[Cr(HPO_3)F_3]$.

Single-Crystal X-ray Diffraction. Prismatic single crystals of the $(C_2H_{10}N_2)[M(HPO_3)F_3]$ compounds with dimensions $0.2 \times 0.04 \times 0.025$ and $0.08 \times 0.035 \times 0.03$ mm for M = V, and Cr, respectively, were carefully selected under a polarizing microscope and mounted on a glass fiber. Diffraction data were collected at room temperature on an Enraf-Nonius CAD4 automated diffractometer for compound (**1**). The data collection of compound (**2**) was performed at 100 K on a Bruker Smart-Apex CCD automated diffractometer. The graphite-monochro-

(8) Serre, C.; Millange, F.; Thouvenot, C.; Nogues, M.; Marsolier, G.; Louer, D.; Ferey, G. *J. Am. Chem. Soc.* **2002**, *124*, 13519.

(9) Fernandez, S.; Mesa, J. L.; Pizarro, J. L.; Lezama, L.; Arriortua, M. I.; Rojo, T. *Angew. Chem., Int. Ed.* **2002**, *41*, 3683.

(10) (a) Guliants, V. V.; Benziger, J. B.; Sundaresan, S. *Chem. Mater.* **1995**, *7*, 1485. (b) Guliants, V. V.; Benziger, J. B.; Sundaresan, S. *Chem. Mater.* **1995**, *7*, 1493.

(11) Powder Diffraction File − Inorganic and Organic, ICDD Files (a) 37-0809 and (b) 27-0948; International Center for Diffraction Data: Newtown Square, PA, 1995.

Table 1. Crystal data, details of data collection, and structure refinement for the $(C_2H_{10}N_2)[M(HPO_3)F_3]$ (M = V and Cr) Phosphites

formula	$C_2H_{11}F_3N_2O_3PV$	$C_2H_{11}F_3N_2O_3PCr$
molecular weight ($gmol^{-1}$)	250.0	251.1
crystal system	orthorhombic	orthorhombic
space group	$P2_12_12_1$ (no. 19)	$P2_12_12_1$ (no. 19)
a, Å	12.809(2)	12.801(2)
b, Å	9.518(1)	9.337(1)
c, Å	6.440(1)	6.508(1)
V, Å^3	785.2(2)	777.9(2)
Z	4	4
$\rho_{calc.}$, gcm^{-3}	2.115	2.144
F(000)	504	508
T, K	293	100
radiation, λ(Mo Kα), Å	0.71073	0.71073
μ (Mo Kα), mm^{-1}	1.493	1.703
limiting indices	$0 < h < 17, 0 < k < 12, 0 < l < 8$	$-16 < h < 15, -12 < k < 9, -8 < l < 8$
R [$I > 2\sigma(I)$]	$R1 = 0.060$ $wR2 = 0.106$	$R1 = 0.057$ $wR2 = 0.117$
R [all data]	$R1 = 0.169$ $wR2 = 0.126$	$R1 = 0.088$ $wR2 = 0.127$
goodness of fit	0.856	0.879

[a] $R1 = [\Sigma(|F_o| - |F_c|)]/\Sigma|F_o|$; $wR2 = [\Sigma[w(|F_o|^2 - |F_c|^2)^2]/\Sigma[w(|F_o|^2)^2]]^{1/2}$; $w = 1/[\sigma^2|F_o|^2 + (xp)^2]$]; where $p = [|F_o|^2 + 2|F_c|^2]/3$; $x = 0.0474$ for V; $x = 0.0495$ for Cr.

mated Mo-Kα radiation was used in both cases. Details of crystal data, intensity collection and some features of the structure refinement are reported in Table 1.

1169 reflections were measured for $(C_2H_{10}N_2)[V(HPO_3)F_3]$ in the range $2.67° \leq \theta \leq 28.69°$, which were considered as independent, with 531 observed applying the criterion $I > 2\sigma(I)$. For $(C_2H_{10}N_2)$ $[Cr(HPO_3)F_3]$ the number of measured reflections was 4588 ($2.70° \leq \theta \leq 28.45°$), with 1776 reflections being independent ($R_{int.} = 0.0521$) and 1100 observed with $I > 2\sigma(I)$. Corrections for Lorentz and polarization effects of compound (**1**) were done and also for absorption with the empirical ψ scan method[12] by using the XRAYACS program.[13] In the case of compound (**2**) an absorption correction based on symmetry equivalent reflections was applied using SADABS.[14] The structures were solved by direct methods (SHELXS 97)[15] and refined by the full-matrix least-squares procedure based on F^2, using the SHELXL 97 computer program[16] belonging to the WINGX software package.[17] The scattering factors were taken from ref 18. All non-hydrogen atoms were assigned anisotropic thermal parameters. The coordinates of hydrogen atoms of the phosphite anion were obtained from difference Fourier maps and those of the ethylenediammonium cation were geometrically placed. Final R factors $R1 = 0.169$ (all data) [w$R2 = 0.126$] for (**1**) and $R1 = 0.088$ (all data) [w$R2 = 0.127$] for (**2**). Maximum and minimum peaks in final difference synthesis were 0.964, −0.989 eÅ^{-3} and 0.673, −0.976 eÅ^{-3} for (**1**) and (**2**) phases, respectively. The goodness of fit on F^2 was 0.856 for (**1**) and 0.879 for (**2**). A simulation based on the $(C_2H_{10}N_2)[M(HPO_3)F_3]$, M = V and Cr single-crystal structures was in excelent agreement with the X-ray powder data, indicating the presence of pure phases with high crystallinity. The structure factor parameters have been deposited at the Cambridge Crystallographic Data Centre (CCDC 197386 and CSD-412497). All drawings were made using the ATOMS program.[19] Fractional atomic coordinates and equivalent isotropic thermal parameters are shown in Table 2. Selected bond distances are given in Table 3.

Table 2. Fractional Atomic Coordinates and Equivalent Isotropic Thermal Parameters (Å^2 × 10^3) for $(C_2H_{10}N_2)[M(HPO_3)F_3]$ (M = V and Cr) (ESD in Parentheses)

atom	*x*/*a*	*y*/*b*	*z*/*c*	U_{eq}[a]
V	0.8060(2)	0.1783(2)	0.8370(5)	13(1)
P	0.7441(2)	0.1620(3)	0.3373(6)	19(1)
F(1)	0.6602(4)	0.1862(7)	0.839(1)	33(2)
F(2)	0.8103(5)	0.3844(5)	0.837(1)	25(1)
F(3)	0.9601(4)	0.1866(6)	0.829(1)	27(1)
O(1)	0.8120(7)	0.183(1)	0.531(1)	24(2)
O(2)	0.8199(6)	−0.0299(7)	0.834(1)	29(2)
O(3)	0.8106(6)	0.185(1)	1.148(2)	36(2)
N(1)	−0.0108(8)	0.969(1)	0.511(1)	27(2)
N(2)	0.1180(8)	1.0297(9)	−0.006(1)	25(2)
C(1)	0.0381(9)	1.051(1)	0.341(2)	29(3)
C(2)	0.0569(9)	0.956(1)	0.160(2)	36(3)
Cr	0.8093(1)	0.6772(1)	0.8389(2)	17(1)
P	0.7450(2)	0.6611(2)	0.3356(4)	37(1)
F(1)	0.6625(3)	0.6801(4)	0.8484(7)	25(1)
F(2)	0.8091(3)	0.8843(4)	0.8447(7)	22(1)
F(3)	0.9603(3)	0.6867(4)	0.8241(7)	23(1)
O(1)	0.8113(4)	0.6838(6)	0.5388(8)	24(1)
O(2)	0.8195(4)	0.4664(4)	0.8327(9)	24(1)
O(3)	0.8176(3)	0.6770(5)	1.1362(9)	25(1)
N(1)	0.8810(5)	1.0285(6)	1.502(1)	24(2)
N(2)	1.0105(4)	0.9775(6)	0.9940(9)	18(1)
C(1)	0.9408(6)	0.9558(6)	1.338(1)	22(2)
C(2)	0.9603(5)	1.0546(6)	1.163(1)	19(2)

[a] $U_{eq} = (1/3)(U_{11} + U_{22} + U_{33})$.

Physicochemical Characterization Techniques. The IR spectra (KBr pellets) were obtained with a Nicolet FT-IR 740 spectrophotometer in the 400−4000 cm^{-1} range. The Raman spectra were recordered in the 200−3000 cm^{-1} range, with a Nicolet 950FT spectrophotometer equipped with a neodymium laser emitting at 1064 nm. Diffuse reflectance spectra were registered at room temperature on a Cary 2415 spectrometer in the 210−2000 nm range. A Bruker ESP 300 spectrometer was used to record the ESR polycrystalline spectra from room temperature to 5.0 K. The temperature was stabilized by an Oxford Instrument (ITC 4) regulator. The magnetic field was measured with a Bruker BNM 200 gaussmeter and the frequency inside the cavity was determined using a Hewlett-Packard 5352B microwave frequency counter. Magnetic mea-

(12) North, A. C. T.; Philips, D. C.; Mathews, F. S. A Semiempirical Method of Absorption Correction. *Acta Crystallogr.* **1968**, *A24*, 351−359.

(13) Chandrasekaran, A. *XRAYACS: Program for Single-Crystal X-ray Data Corrections*; Chemistry Department, University of Massachusetts: Amherst, MA, 1998.

(14) (a) Blessing, R. H. *Acta Crystallogr.* **1995**, *A51*, 33−38. b) SADABS: Area-Detector Absorption Correction; Bruker-AXS: Madison, WI, 1996.

(15) Sheldrick, G. M. *SHELXS 97: Program for the Solution of Crystal Structures*; University of Göttingen: Germany, 1997.

(16) Sheldrick, G. M. *SHELXL 97: Program for the Refinement of Crystal Structures*; University of Göttingen: Germany, 1997.

(17) Farrugia, L. J. *WINGX. Version 1.63.02: An Integrated System of Windows Programs for the Solution, Refinement and Analysis of Single-Crystal X-ray Diffraction Data. J. Appl. Crystallogr.* **1999**, *32*, 837−838.

(18) *International Tables for X-ray Crystallography*. Kynoch Press: Birmingham, U.K., 1974; Vol. IV, p 99.

(19) Dowty, E. ATOMS: *A computer program for displaying atomic structures;* Shape Software (521 Hidden Valley Road): Kingsport, TN, 1993.

Table 3. Selected Bond Distances (Å) for $(C_2H_{10}N_2)[M_3(HPO_3)_4]$ (M = V and Cr) (ESD in Parentheses)

VO_6 octahedron		CrO_6 octahedron	
V−F(1)	1.869(6)	Cr−F(1)	1.880(3)
V−F(2)	1.962(6)	Cr−F(2)	1.934(4)
V−F(3)	1.976(6)	Cr−F(3)	1.938(3)
V−O(1)	1.972(8)	Cr−O(1)	1.954(5)
V−O(2)	1.990(8)	Cr−O(2)	1.974(4)
V−O(3)	2.01(1)	Cr−O(3)	1.938(5)
HPO_3 tetrahedron		HPO_3 tetrahedron	
P−O(1)	1.535(9)	P−O(1)	1.586(5)
P−O(2)^{i}	1.502(8)	P−O(2)^{ii}	1.448(5)
P−O(3)^{ii}	1.50(1)	P−O(3)^{i}	1.603(6)
P−H(1)	1.32(2)	P−H(1)	1.42(7)
	$(H_3N(CH_2)_2NH_3)^{2+}$		
N(1)−C(1)	1.48(2)	N(1)−C(1)	1.48(1)
C(1)−C(2)	1.49(2)	C(1)−C(2)	1.48(1)
	Intermetallic M−M		
V(1)−V(2)^{iii}	4.894(4)	Cr(1)−Cr(2)^{iii}	4.883(2)
V(1)−V(2)^{iv}	6.440(5)	Cr(1)−Cr(2)^{iv}	6.508(2)

[a] Symmetry codes: $i = -x + 3/2, -y, z - 1/2$; $ii = x, y, z - 1$; $iii = 3/2 - x, -y, z - 1/2$; $iv = x, y, z + 1$.

surements on powdered sample were performed in the temperature range 2.0−300 K, using a Quantum Design MPMS-7 SQUID magnetometer. The magnetic field was approximately 0.1 T, a value in the range of linear dependence of magnetization vs magnetic field even at 2.0 K.

Results and Discussion

Crystal Structure of the $(C_2H_{10}N_2)[M(HPO_3)F_3]$ (M = V and Cr) Compounds. The crystal structure of the $(C_2H_{10}N_2)[M(HPO_3)F_3]$ M = V(III) and Cr(III) compounds consists of $[M(HPO_3)F_3]^{2-}$ anionic chains running along the [001] direction, in which the +III oxidation state of the metallic cations is stabilized by the fluorine anions. The ethylenediammonium cations are displayed in the cavities of the structure delimited by three different chains (Figure 2a). The organic cations establish both hydrogen bonds and ionic interactions with the anionic chains.

The $[M(HPO_3)F_3]^{2-}$ chains are constructed from MO_3F_3 isolated octahedra and pseudopyramidal $(HPO_3)^{2-}$ phosphite oxoanions (Figure 2b). The MO_3F_3 octahedra share the *trans*-O(1),O(3) atoms with the $HP(1)O_3$ tetrahedra, forming an infinite chain of alternating octahedra and tetrahedra. Each octahedron also shares the O(2) atom from another $HP(1)O_3$ tetrahedron belonging to a parallel identical chain, giving rise to infinite zigzag chains as shown in Figure 2b. A remarkable structural feature of this compound is the absence of covalent intrachain −M−O,F−M− interactions.

The metallic cations of the MO_3F_3 octahedra in the title compounds are bonded to the O(1), O(2), and O(3)-oxygen atoms belonging to the HPO_3 anion, and to the F(1), F(2) and F(3)-fluorine ions. For compound (**1**) the V−O,F bonds are in the range 1.869(6)−2.01(1) Å, whereas the cis and trans angles range from 86.1(3)° to 97.5(3)° and from 173.2(3)° to 175.3(3)°, respectively. In compound (**2**) the Cr−O,F distances vary from 1.880(3) to 1.974(4) Å, and the cis and trans angles are in the 86.3(2)−94.7(2)° and 175.7(2)−176.4(2)° ranges, respectively. The M^{III}−M^{III} intrachain bond distances, along the *c* axis and the zigzag pathway, are 4.894(4), 6.440(5) Å and 4.883(2), 6.508(2) Å, for compounds (**1**) and (**2**), respectively. The mean P−O bond distance is 1.46(9) Å for (**1**) and 1.55(8) Å for (**2**). The O−P−O and H−P−O angles show values usually found in tetrahedral coordination. In these compounds the ethylenediammonium cations establish strong hydrogen bonds with the oxygen atoms from the phosphite anion and the fluorine ions.

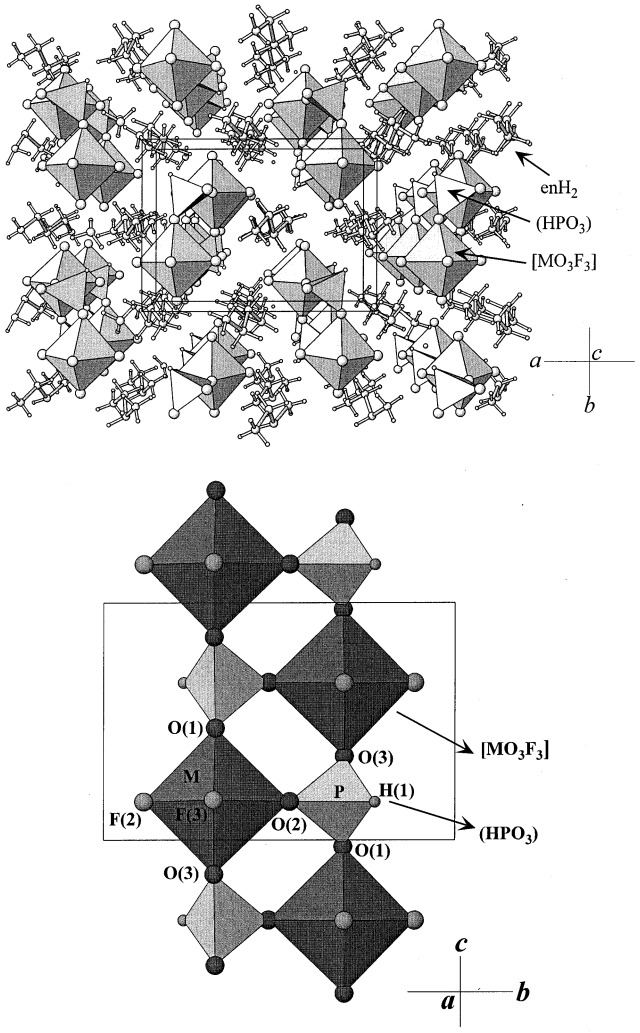

Figure 2. Polyhedral view of (a) the crystal structure of the $(C_2H_{10}N_2)[M(HPO_3)F_3]$ (M = V and Cr) compounds; and (b) a zigzag chain along the *c* axis.

Spectroscopic Properties. The infrared and Raman spectra of the $(C_2H_{10}N_2)[M(HPO_3)F_3]$ (M = V and Cr)

Table 4. Selected Bands (Values in cm^{-1}) from the IR and Raman Spectra for the $(C_2H_{10}N_2)[M(HPO_3)F_3]$ (M = V and Cr) Compounds

	M = V		M = Cr	
assignment	IR	Raman	IR	Raman
$\nu(-NH_3)^+$	3165, 3040 (s)[a]	3015, 2980 (s)	3195, 3050 (s)	3020, 2985 (s)
$\nu(-CH_2-)$	2945−2455 (w)	2860−2840 (m)	2950−2460 (w)	2945−2840 (m)
ν(HP)	2380 (m)	2375 (s)	2375 (m)	2385 (s)
$\delta(-NH_3)^+$	1535 (s)	1550 (w)	1540 (s)	1510 (w)
$\delta(-CH_2-)$	1480−1350 (w)	1460−1345 (w)	1500−1320 (w)	1490−1400 (w)
$\nu_{as}(PO_3)$	1170 (s)	1100 (m)	1175 (s)	1065 (m)
δ(HP)	1080 (s)	1060 (s)	1050 (m)	1050 (s)
$\nu_s(PO_3)$	1025 (s)	920 (m)	1025 (s)	930 (m)
$\delta_s(PO_3)$	595 (m)	540 (w)	605 (m)	590 (w)
$\delta_{as}(PO_3)$	505 (m)	480 (w)	530 (m)	475 (w)

[a] ν = stretching, δ = deformation, s = symmetric, as = asymmetric, s = strong, m = medium, w = weak.

phases exhibit in all cases the bands corresponding to the vibrations of the ethylenediammonium cations and the $(HPO_3)^{2-}$ phosphite anions. Selected bands obtained from both the IR and Raman spectra are given in Table 4. It is worth mentioning the presence of the vibrational modes of the protonated ethylenediamine molecule, in agreement with the structural data. These results are similar to those found for other ethylenediammonium phases.[20]

The reflectance diffuse spectrum of $(C_2H_{10}N_2)[V(HPO_3)F_3]$ shows the spin allowed transitions from the fundamental state $^3T_{1g}(^3F)$ to the excited levels $^3T_{2g}(^3F)$, $^3T_{1g}(^3P)$, and $^3A_{2g}(^3F)$ at frequencies 14445, 21580, and 30025 cm^{-1}, respectively. Furthermore, the spin forbidden transition $^3T_{1g}(^3F) \rightarrow {}^1E_g(^1D)$, $^1T_{2g}(^1D)$ was observed as a shoulder on the first band at 9770 cm^{-1}. The *Dq* and Racah (*B* and *C*) parameters were calculated by fitting the experimental frequencies to the energy expressions for a d^2 ion.[21a] The values are $Dq = 1560$ cm^{-1}, $B = 550$ cm^{-1}, and $C = 3060$ cm^{-1}. In the case of $(C_2H_{10}N_2)[Cr(HPO_3)F_3]$ the reflectance diffuse spectrum shows the spin allowed transitions from the fundamental state $^4A_{2g}(F)$ to the excited levels $^4T_{2g}(^4F)$, $^4T_{1g}(^4F)$, and $^4T_{1g}(^4P)$ at the frequencies 15505, 22220, and 34485 cm^{-1}, respectively. Furthermore, the spin forbidden transitions $^4A_{2g}(F) \rightarrow {}^2E_g(^2G)$, $^2T_{1g}(^2G)$ were observed as shoulders on the first band at 14770 and 16075 cm^{-1}, respectively. The *Dq* and Racah parameters for this d^3 cation are $Dq = 1535$ cm^{-1}, $B = 720$ cm^{-1}, and $C = 3280$ cm^{-1}.

The values obtained for the *Dq* and Racah parameters are in good agreement with those observed for the V(III) and Cr(III) ions in octahedral environment.[21] The *B* parameter is approximately 65% for compound (**1**) and 75% for compound (**2**) of that corresponding to the V^{3+} and Cr^{3+} free ions (861 or 918 cm^{-1}, respectively), which indicates the existence of a significant covalence character in the V,Cr−O,F chemical bonds.

ESR and Magnetic Properties. The ESR spectra of $(C_2H_{10}N_2)[Cr(HPO_3)F_3]$ were recorded on powdered sample at *X* band between 4.2 and 300 K. The spectra

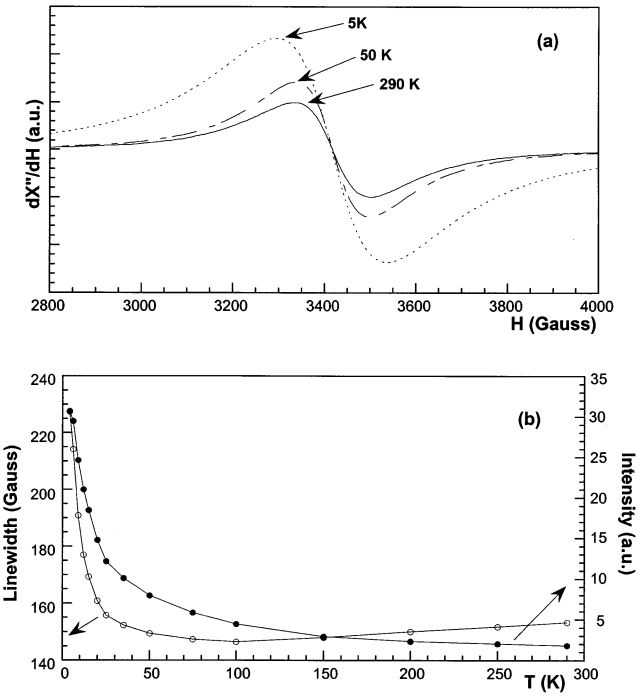

Figure 3. (a) Powder X-band ESR spectra of $(C_2H_{10}N_2)[Cr(HPO_3)F_3]$ at different temperatures. (b) Temperature dependence of the intensity of the signal and the line width curves.

remain essentially unchanged upon cooling the sample from 300 to ca. 50 K (Figure 3a). Below this temperature the signal broadens and increases its intensity. The spectra are isotropic with a "*g*" value of 1.97, which remains unchanged with variation in temperature. This *g* value is characteristic of slightly distorted octahedral coordinated Cr(III) ions. The temperature dependence of the intensity and the line width of the signals calculated by fitting the experimental spectra to Lorentzian curves are displayed in Figure 3b. The intensity of the signal increases in the temperature range studied, and does not exhibit any substantial decrease at low temperatures. This behavior could be explained by considering the compound as either a paramagnetic or an antiferromagnetic system in which the maximum in the magnetic susceptibility appears at temperatures lower than 5.0 K, the minimum operating temperature of the ESR spectrometer used in the experiment. The line width of the ESR signals remains practically unchanged from room temperature to ca. 50 K, and after that the line width vigorously increases due to the existence of a strong spin correlation.[22−26]

(20) (a) Gharbi, A.; Jouini, A.; Averbuch-Pouchot, M. T.; Durif, A. *J. Solid State Chem.* **1994**, *111*, 330. (b) Dolphin, D.; Wick, A. E. *Tabulation of Infrared Spectral Data;* John Wiley & Sons: New York, 1977. (c) Tsuboi, M. *J. Am. Chem. Soc.* **1957**, *79*, 1351. (d) Nakamoto, K. *Infrared and Raman Spectra of Inorganic and Coordination Compounds;* John Wiley & Sons: New York, 1997.

(21) (a) Lever, A. B. P. *Inorganic Electronic Spectroscopy,* Elsevier Science Publishers B. V.: Amsterdam, The Netherlands, 1984. (b) Mason, W. R.; Gray, H. B. *J. Am. Chem. Soc.* **1968**, *90*, 5721. (c) Sutton, J. E.; Krentzien, H.; Taube, H. *Inorg. Chem.* **1980**, *19*, 2425.

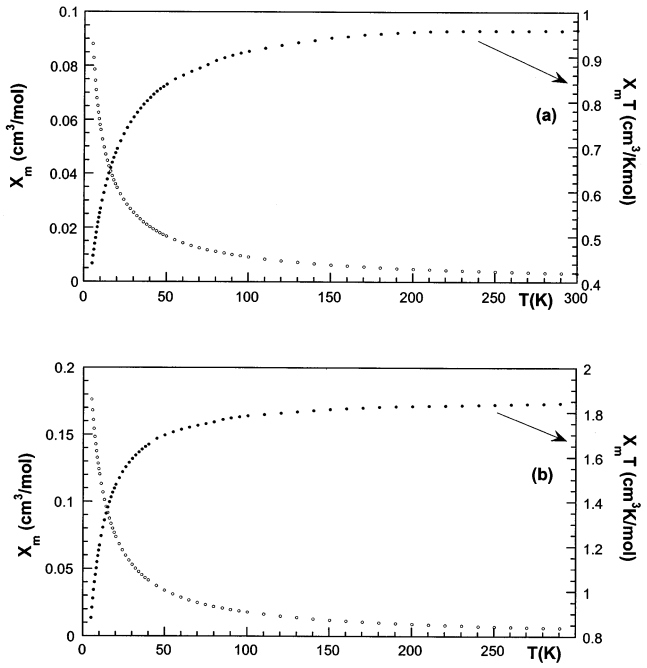

Figure 4. Thermal evolution of χ_m and $\chi_m T$ curves of the (a) vanadium and (b) chromium.

Magnetic measurements of $(C_2H_{10}N_2)[M(HPO_3)F_3]$ (M = V and Cr) were performed on powdered samples from room temperature to 2.0 K. Plots of χ_m and $\chi_m T$ curves are shown in Figure 4.

The molar magnetic susceptibility of the vanadium and chromium compounds increases with decreasing temperature in all the temperature range studied (Figure 4). The thermal evolution of χ_m of these compounds follows the Curie−Weiss law at temperatures higher than 50 K. The calculated Curie and Curie−Weiss constants are $C_m = 0.99$ cm^{3}K/mol, $\theta = -8.1$ K for (**1**) and $C_m = 1.88$ cm^{3}K/mol, $\theta = -5.4$ K for (**2**). The negative Weiss temperature and the continuous decrease of the $\chi_m T$ product from room temperature to 2.0 K indicate the existence of antiferromagnetic interactions in these compounds. Considering the structural features of these compounds, the connection between the vanadium(III) or chromium(III) paramagnetic cations takes place along the M−O−P−O−M exchange pathways that favor the antiferromagnetic interactions as was observed in other related compounds.[27]

Concluding Remarks

Two new inorganic−organic hybrid materials based on vanadium(III) and chromium(III) cations and the $(HPO_3)^{2-}$ phosphite oxoanion have been synthesized by using mild hydrothermal reactions. The inorganic framework of these compounds adopts a zigzag chain structure. The templating ethylenediamine molecules are located between the chains, and establish both ionic interactions and hydrogen bonds with the inorganic skeleton. After the loss of the ethylenediammonium cations the crystal structure of the compounds collapses. The spectroscopic data in the visible region confirm the presence of the metallic cations in slightly distorted octahedral geometry. The ESR measurements for the chromium phase show an isotropic *g* tensor, which remains unchanged with variation in temperature. The thermal evolution of the intensity of the ESR spectra until 5.0 K can be associated with a paramagnetic or antiferromagnetic system. The magnetic measurements of these compounds indicate the existence of antiferromagnetic interactions, which are propagated via the phosphite anions.

Acknowledgment. This work was financially supported by the Ministerio de Educación y Ciencia (BQU2001-0678) and Universidad del País Vasco/ EHU (9/UPV00169.310-13494/2001; 9/UPV00130.310-13700/2001), which we gratefully acknowledge. S.F. thanks the Gobierno Vasco/Eusko Jaurlaritza for a doctoral fellowship.

Supporting Information Available: Listing of details of the X-ray single-crystal diffraction structural resolution (CIF). This material is available free of charge via the Internet at http://pubs.acs.org.

CM021361B

(22) Wijn, H. W.; Walker, L. R.; Daris, J. L.; Guggenheim, H. *J. Solid Sate Commun.* **1972**, *11*, 803.
(23) Richards, P. M.; Salamon, M. B. *Phys. Rev. B* **1974**, *9*, 32.
(24) Escuer, A.; Vicente, R.; Goher, M. A. S.; Mautner, F. *Inorg. Chem.* **1995**, *34*, 5707.
(25) Bencini, A.; Gatteschi, D. *EPR of Exchange Coupled Systems*; Springer-Verlag: Berlin/Heidelberg, 1990.
(26) Cheung, T. T. P.; Soos, Z. G.; Dietz, R. E.; Merrit, F. R. *Phys. Rev. B* **1978**, *17*, 1266.
(27) Lezama, L.; Suh, K. S.; Villeneuve, G.; Rojo, T. *Solid State Commun.* **1990**, *76*, 449.